



OPEN ACCESS

EDITED BY

Vikrant Sudan,
Guru Angad Dev Veterinary and Animal
Sciences University, India

REVIEWED BY

Amit Singh,
Narendra Dev University of Agriculture and
Technology, India
Remil Galay,
University of the Philippines Los Baños,
Philippines

*CORRESPONDENCE

Mohammed Barham
✉ barham.mohammed@uk-koeln.de

[†]These authors have contributed equally to this work

RECEIVED 23 June 2023

ACCEPTED 11 September 2023

PUBLISHED 28 September 2023

CITATION

Nawshirwan S, Heucken N, Piekarek N, van Beers T, Fulgham-Scott N, Grandoch A, Neiss WF, Vogt J and Barham M (2023) Morphological, ultrastructural, genetic characteristics and remarkably low prevalence of macroscopic *Sarcocystis* species isolated from sheep and goats in Kurdistan region, Iraq. *Front. Vet. Sci.* 10:1225796. doi: 10.3389/fvets.2023.1225796

COPYRIGHT

© 2023 Nawshirwan, Heucken, Piekarek, van Beers, Fulgham-Scott, Grandoch, Neiss, Vogt and Barham. This is an open-access article distributed under the terms of the [Creative Commons Attribution License \(CC BY\)](https://creativecommons.org/licenses/by/4.0/). The use, distribution or reproduction in other forums is permitted, provided the original author(s) and the copyright owner(s) are credited and that the original publication in this journal is cited, in accordance with accepted academic practice. No use, distribution or reproduction is permitted which does not comply with these terms.

Morphological, ultrastructural, genetic characteristics and remarkably low prevalence of macroscopic *Sarcocystis* species isolated from sheep and goats in Kurdistan region, Iraq

Salh Nawshirwan^{1†}, Nicole Heucken^{2†}, Nadin Piekarek³,
Tim van Beers⁴, Nicole Fulgham-Scott⁵, Andrea Grandoch⁵,
Wolfram F. Neiss⁴, Johannes Vogt^{2,6} and Mohammed Barham^{2*}

¹Directorate of Veterinary Medicine, Sulaymaniyah, Iraq, ²Department II of Anatomy, Faculty of Medicine, University Hospital Cologne, Cologne, Germany, ³Experimental Medicine, Faculty of Medicine, University Hospital Cologne, Cologne, Germany, ⁴Department I of Anatomy, Faculty of Medicine, University Hospital Cologne, Cologne, Germany, ⁵Department for Oral and Craniomaxillofacial and Plastic Surgery, Faculty of Medicine, University of Cologne and University Hospital of Cologne, Cologne, Germany, ⁶Cluster of Excellence for Aging Research (CECAD) and Center of Molecular Medicine Cologne (CMMC), University of Cologne, Cologne, Germany

Introduction: *Sarcocystis* is a genus of cyst-forming parasites that infest both humans and livestock. Some parasites cause clinical and subclinical diseases in their hosts, resulting in economic losses.

Methods: Esophagus, diaphragm, and skeletal muscle from slaughtered sheep and goats were examined macroscopically, microscopically, and ultrastructurally and subjected to DNA analysis.

Results: We isolated macrocysts of *S. gigantea* and of *S. capraefelis moulei* from naturally infected sheep (*Ovis aries*) and goats (*Capra hircus*). The macrocyst wall thickness was 18.9 μm in sheep and 15.3 μm in goats, and consisted of an inner Periodic acid Schiff- (PAS) negative primary wall and an outer glycoconjugates containing i.e. PAS-positive secondary wall. The walls inner surface was compartmentalized and filled with bradyzoites. In *S. gigantea* the bradyzoites were approximately 12.3 x 2.6 μm in size, while in *S. capraefelis moulei* they were 13.9 x 4.4 μm . Ultrastructurally, both species have nearly identical morphology: cauliflower-like protrusions with numerous microtubules and often dendritic-like filaments, branching from the primary wall. The 18S rRNA gene in *S. gigantea* was 85.9% identical to that in *S. medusiformis* and 80.4% to the *S. capraefelis moulei* gene. The 28S rRNA gene in *S. gigantea* was 94.6% identical to that in *S. medusiformis* and 97.3% to the *S. capraefelis moulei*.

Conclusion: This study is the first to (i) detail the ultrastructure of the macrocyst wall of *S. capraefelis moulei*, (ii) identify *S. medusiformis* in Iraqi sheep, and (iii) compare the prevalence of macroscopic *Sarcocystis* at different time periods within the same region. A positive finding was the reduction of macroscopic sarcocystosis occurrences (0.01% in sheep and 0.02% in goats) compared to our previous data from 1992 (4.1%: sheep, 33.6%: goats).

KEYWORDS

genetic analysis, goat, sheep, *Sarcocystis gigantea*, *Sarcocystis medusiformis*, *Sarcocystis moulei*

1. Introduction

Sarcocystis species are coccidian parasites, belonging to the phylum: Apicomplexa, class: Conoidasida, order: Eucoccidiorida, and family: Sarcocystidae (1). They are distributed worldwide and parasitic to a broad range of vertebrates, such as cattle, sheep and goats. *Sarcocystis* spp. have also been isolated in Europe: Germany (2) Lithuania (3), Italy (4), the Netherlands (5) and Spain (6). Sheep are intermediate hosts for at least four species of *Sarcocystis*: *S. gigantea* (syn. *S. ovifelis*), *S. medusiformis*, *S. tenella* and *S. arieticanis*. Both species, *S. gigantea* and *S. medusiformis* are transmitted through felids and produce macrocysts. *S. tenella* and *S. arieticanis*, on the other hand, are transmitted through canids and produce microcysts (1, 7, 8). Infections from *S. tenella*, *S. gigantea* and *S. arieticanis* are common worldwide, whereas *S. medusiformis* infections have been exclusively reported in Australia, New Zealand, Iran and Italy (4, 9).

Goats are intermediate hosts for at least three *Sarcocystis* species: *S. capracanis*, *S. hircicanis*, and *S. caprafelis moulei*. *S. capracanis* and *S. hircicanis* are transmitted through canids [review (1)], and generally produce microcysts. On the other hand, *S. caprafelis moulei* [termed *S. moulei* (10–12)] is transmitted by felids and produces macrocysts (1).

The prevalence of macroscopic sarcocystosis in domestic sheep varied regionally: 4.1% in Iraq (13), 29.3% in Iran (14), and 42.7% in Egypt (15). In domestic goats macrocysts occurred 33.6% in Kurdistan/Iraq (11), 16.6% in Iran (16) and 35.5% in Egypt (15). There is but a single, brief description of the *S. moulei* macrocysts ultrastructure in Egyptian goats (17). In comparison, many studies described the localization, the pathogenesis, the cyst wall and bradyzoites structure and ultrastructure, as well as the *S. gigantea* DNA analysis in both natural and experimentally-infected sheep (1, 13, 18).

This study aims to identify *Sarcocystis* species isolated from muscle macrocysts from naturally infected domestic sheep and goats. In addition, we compare the prevalence of macroscopic sarcocystosis in the same region at different time periods. Finally, we demonstrate the differences in macro- and microscopic structure, ultrastructural morphology, and genetic characterization of macrocysts between *S. gigantea* and *S. caprafelis moulei*. To our knowledge, this is the first study (i) to describe the macrocyst wall structure using PAS-staining, (ii) to study in detail the ultrastructure of macrocysts, including protrusions and filaments of *S. caprafelis moulei* in goats, and (iii) to demonstrate isolates of *S. medusiformis* in domestic sheep in Iraq.

2. Materials and methods

2.1. Animals

A total of 141,260 domestic sheep (*Ovis aries*; 98,638 male and 42,622 female) and 37,399 domestic goats (*Capra hircus*; 32,441 male and 4,958 female) were slaughtered and investigated between September 2021 and March 2022 in 6 regional abattoirs (Sulaimany, PiraMagroon, Khalakan, Darbandixan, Takya and Soran) in the northern Iraq Kurdistan region (Supplementary material S1). All slaughtered animals were carefully inspected by specialist personal and in case of any pathological changes reinspected by veterinarians. If *Sarcocystis* macrocysts were detected in esophagus, diaphragm or skeletal muscles, all obvious macrocysts and the surrounding muscle

tissue were collected, and age (as estimated by dental examination) and sex of the respective animal were recorded. All tissue sampling was performed under the supervision and with permission of the state veterinarian in the above-mentioned slaughterhouses. Written consent from the animal's owners for the participation of their animals in this study was not required in accordance with the national legislation and the institutional requirements.

2.2. *Sarcocystis* macrocysts

Out of a total of 141,260 sheep, only 20 had *Sarcocystis* macrocysts, and out of a total of 37,399 goats only nine carried *Sarcocystis* macrocysts, all of which were embedded in the muscular tissue and were milky-white and grainy in appearance. All 29 infected animals appeared healthy and showed no signs of disease before slaughter. Of the 20 infected sheep, we collected 21 pieces of infected tissue: 11 from skeletal muscle, five from the diaphragm, and five from the esophagus, namely one sheep had macrocysts in both skeletal muscle and esophagus. Of the nine infected goats, 12 tissue pieces were collected, nine from the esophagus and three from skeletal muscle. Here, three goats exhibited macrocysts in both the esophagus and skeletal muscle. Each tissue piece contained a minimum of two and a maximum of 12 *Sarcocystis* macrocysts. The size of *Sarcocystis* macrocysts in sheep and goats were then measured using a digital caliper. Tissue pieces from esophagus and skeletal muscle containing macrocysts were randomly divided into three groups, and then immediately fixated by immersion in the following solutions: 4% paraformaldehyde (PFA) in 0.1 M phosphate buffer pH 7.4 for histological examination, 70% ethanol for DNA purification, and sequencing or 2% glutaraldehyde (GLA) plus 2% PFA in 0.1 M phosphate buffer pH 7.4 for transmission electron microscopy.

2.3. Histological examination

Ten of the 21 macrocysts-containing sheep samples, and four of the 12 macrocysts-containing goat samples were fixed in 4% buffered formaldehyde, embedded in paraffin, serially sectioned at 5 µm thickness with a rotary microtome (Leica Autocut 1,140). The slides containing tissue sections were then stained with Tri-PAS (30 min 1% Periodic acid at room temperature 10 min Schiff's reagent (19) Mayer's hematoxylin and methylene blue. All samples were further imaged with a Zeiss AX10 light microscope and a Hitachi HV-F202 camera. The following measurements were all measured using image analysis software Image-Pro® Plus version 6.0 (Media Cybernetics, Inc. MD 20910, United States): (i) thickness of the degenerating layer, primary and secondary cyst walls, villous protrusions, and internal cyst compartments, and (ii) bradyzoites dimensions.

2.4. Transmission electron microscopy

Twelve *Sarcocystis* macrocysts from sheep and four from goats were collected from the esophagus and skeletal muscles and immersion-fixed at 4°C in a solution containing 2% GLA plus 2% PFA in 0.1 M Phosphate buffer, pH 7.4, and left in solution for up to 2 weeks for logistical reasons. After nine rinses in 0.1 M cacodylate buffer pH

7.4, the cysts were postfixed for 2 h with 1% OsO₄ + 1.5% K₃Fe₃ (CN)₆ in 0.1 M cacodylate buffer, pH 7.4 (20, 21). The tissues were dehydrated *via* acetone/propylene oxide and embedded in epoxide resin (epon; Fluka, Switzerland).

For morphometric light microscopical analysis, 0.5 μm thick cross sections of epoxide embedded cysts were stained with methylene blue. Ultrathin sections (30 nm) were cut with a diamond knife, mounted on formvar/carbon-coated 200-mesh copper grids and contrasted with uranyl acetate and lead citrate solution. TEM was performed with a Zeiss EM109 (80 kV, 200 μm condenser and 30 μm objective apertures, TRS-2K-Camera). Magnification of micrographs was calibrated by means of a cross-grating replica (2,160 lines/mm; Polaron, England).

To analyze morphology, methylene blue stained semithin sections of several macrocysts were imaged with a Zeiss AX10 light microscope. For the investigation of cyst wall morphology, villous protrusions, and bradyzoites, the length and width of these *Sarcocystis* components were measured using the same image analysis software as for paraffin sections (see above).

2.5. DNA purification

The collected macrocysts from sheep ($n=10$) and goats ($n=4$) were stored in 70% ethanol until DNA extraction. The samples were briefly lysed in lysis buffer (200 mM Tris pH8, 50 mM EDTA pH8; 100 mM NaCl, 1% SDS in H₂O), supplemented with 30 U/mg Proteinase K at 600 rpm and 55°C overnight. The following day, samples were centrifuged 8 min at 14000 rpm to separate the genomic DNA in the supernatant from cell debris in the pellet. The supernatant was transferred to fresh tubes containing 500 μL ice cold 100% EtOH resulting in DNA filaments to form. For washing, the DNA filaments were collected with a Pasteur pipette tip from the liquid and transferred into a new tube containing 375 μL ice cold 70% EtOH. Finally, DNA was resuspended in 75 μL ultra pure nuclease-free water overnight at 42°C and stored at 4°C until further analysis.

2.6. PCR amplification, gel extraction and DNA sequencing

New primers for amplification of the 18S rRNA and 28S rRNA genes were designed, so that one primer pair each could be used to amplify the gene of interest from all of the mentioned species (*S. gigantea*, *S. medusifformis* and *S. caprafelis moulei*). Therefore, the reference sequences for either the 18S rRNA or 28S rRNA genes of *S. gigantea*, *S. medusifformis* and *S. caprafelis* were aligned. Primer binding sites were selected in sections where all three reference sequences have 100% sequence identity and surrounding sections where the sequences had the greatest differences between the three named species. The primer pair oBM001 (5'-ACTGCGAATGGCTCATTTAAACA-3'), and oBM002 (5'-TGATCGTCTTCGAGCCCCCTA-3') amplified a fragment between 1,001 bp and 1,072 bp from the 18S rRNA gene of each species. For the 28S rRNA, the primers oBM003 (5'-AGCGGTGGAGAAGAAAATAACA-3') and oBM004 (5'-TCACATGGAACCCTTCTCCA-3') resulted in a fragment of 1,674 bp, 1,676 bp, and 1,680 bp, respectively.

PCR amplification was performed in a thermocycler using the following program for 18S rRNA: Initial denaturation at 95°C (3 min), followed by 30 cycles of 95°C (30s), 60°C (30s) and 72°C (70s), ending with a final elongation at 72°C (5 min). For the 28S rRNA, the program differed slightly: Initial denaturation at 95°C (3 min), followed by 30 cycles of 95°C (30s), 58°C (30s) 72°C (1 min and 45 s), ending with a final elongation at 72°C (5 min).

PCR products were run on a 1% agarose gel together with GeneRuler 100 bp and 1 kb plus DNA ladders (ThermoFischer), stained with 0,1 μg/mL Ethidiumbromide, and further analyzed after electrophoresis with a UV transilluminator. Proportionally correct bands were excised from the gel and underwent DNA extraction using the NucleoSpin Gel and PCR Clean-up kit (Macherey-Nagel), according to the manufacturer's instructions.

For each Cyst, one PCR product per gene of interest was sequenced with forward and reverse primers for the respective gene in two individual reactions.

Sequencing results were obtained from Microsynth Seqlab¹ and analyzed in SnapGene and with the NCBI Blast Tool.²

2.7. Sequence databases

Nucleotide sequences referred to as reference sequences or BLAST results mentioned in this paper are available in the GenBank™ NCBI nucleotide databases under the accession numbers: MK420020.1, MK420025.1, MK420021.1, MK420026.1, L76473.1, AF012884.1, KP053891.1, MK045326.1, and GQ131808.1. All our data sequences for 18S rRNA and 28S rRNA genes are deposited in NCBI under the accession numbers (see [Supplementary material S1](#)).

2.8. Statistical evaluation

All values (dimensions of macrocysts, bradyzoites and villar protrusions, thickness of cyst walls and degenerating layers) are expressed as the mean ± s.e.m. (standard error of the mean). Following outlier analysis, two group comparisons were performed using an unpaired two-tailed *t*-test for normal distributed data and a Mann-Whitney test for nonparametric data. Corresponding details are given in the figure legend. Analysis were performed using GraphPad Prism 9.2.0. Statistical significance was considered at $p < 0.05$ and marked with *, $p < 0.01$ was assigned with **, $p < 0.001$ with ***, and $p < 0.0001$ with ****.

3. Results

3.1. Macroscopic characterization

Out of a total of 141,260 sheep, and 37,399 goats ([Supplementary material S1](#)) slaughtered and subsequently examined by veterinarians, only 20 sheep (0.01%) and nine goats (0.02%)

¹ <https://srvweb.microsynth.ch/>

² <https://blast.ncbi.nlm.nih.gov/Blast.cgi>

contained *Sarcocystis* macrocysts. *S. gigantea* and *S. capraefelis moulei* fresh, unfixed macrocysts appeared milky-white and grainy and were always found embedded in muscle tissue. *S. gigantea* macrocysts (Figure 1) appeared large, thick, round or elongated. They were located exclusively in the diaphragm and esophagus with an average length of 6.7 mm and width of 2.9 mm. Further, *S. capraefelis moulei* macrocysts (Figure 1D; Supplementary material S2) seemed also large, thick, oval or round; they were exclusively found in the esophagus—preferentially in the lower half—with an average length of 6.3 mm and width of 4.0 mm (Figures 2A,B; Supplementary material S2). A two-tailed *t*-test revealed no significant difference ($p < 0.05$) in macrocyst length, but a significant difference ($p < 0.01$) in macrocyst width (Figures 2A,B) between sheep and goats. This mean difference of 2.9 mm versus 4.0 mm macrocyst width is not, however, reliably discernible by observation. The macroscopic identification of *S. gigantea* and *S. capraefelis moulei* depends solely on the source of the

sample: *S. gigantea* is collected from sheep, *S. capraefelis moulei* from goats. Evidence that these truly are different macrocyst subspecies is provided only by DNA sequencing and ultrastructural analysis (see below). All structures, that were deemed macrocysts by macroscopical inspection, proved to be so by histological, electron microscopical or DNA analysis.

3.2. Lightmicroscopic characterization

In histological sections of muscle tissues, the macrocysts were thick-walled and consisted of two layers in both species. The mean wall thickness was 18.9 μm in *S. gigantea* and was 15.3 μm in *S. capraefelis moulei* (Figure 2E). An outer PAS-positive, i.e., covalently bound glycoconjugates containing secondary thick wall (11.6 μm in sheep; 8.0 μm in goats) was stained purple-red in Figures 1B,E, 2D. And an

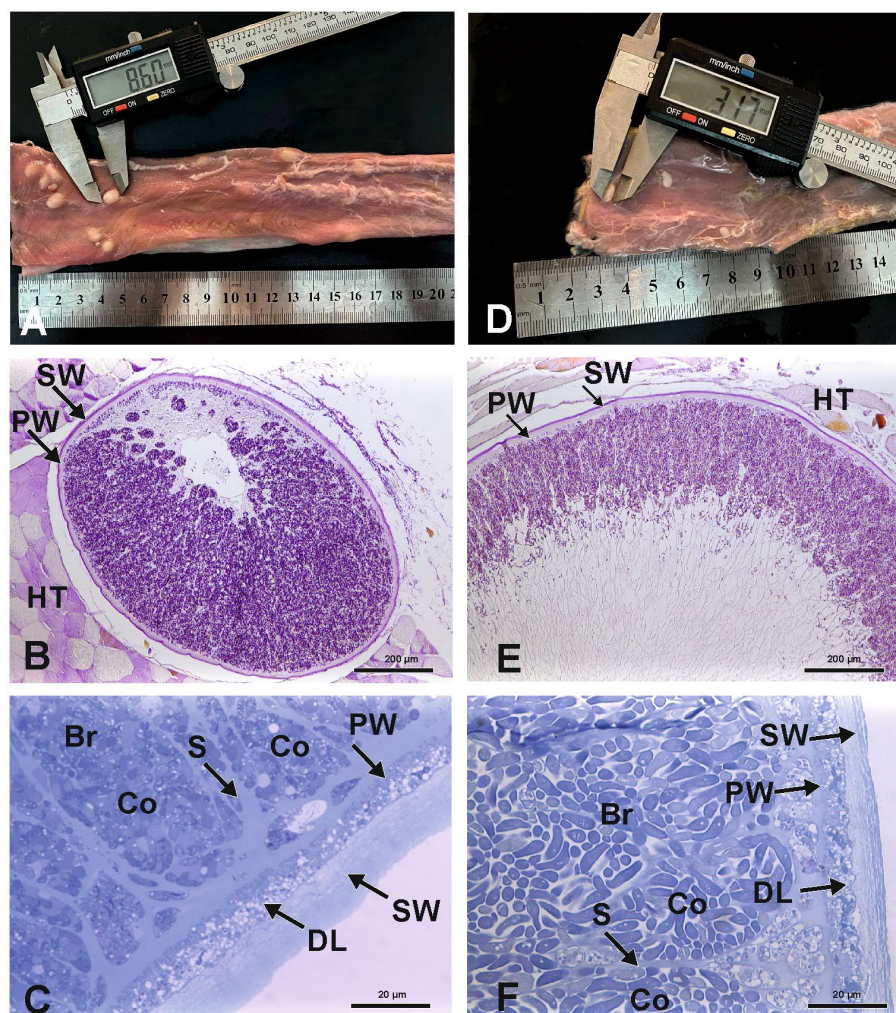


FIGURE 1

Macroscopy and light microscopy of *S. gigantea* (A–C) and *S. capraefelis moulei* (D–F) macrocysts. Gross appearance of macrocysts of *S. gigantea* in sheep (A) and *S. capraefelis moulei* in goat (D) in the heavily infected esophagi, scale bar in cm. Light microscopic appearance of an oval macrocyst of *S. gigantea* (B) and *S. capraefelis moulei* (E), both macrocysts have a PAS-positive outer secondary thick wall (SW), and a PAS-negative inner primary relatively thick wall (PW), HT = Host tissue. Higher magnification shows the primary and secondary walls of the macrocysts of *S. gigantea* (C) and *S. capraefelis moulei* (F). Between the primary and secondary walls is a relatively thick layer of degenerating host cells (DL). Beneath the primary wall are numerous compartments (Co) separated by tissue septa (S) and filled with banana-shaped bradyzoites (Br), (B) and (E) 5 μm paraffin sections, Tri-PAS staining; (C) and (F) 0.5 μm semithin sections, methylene blue staining.

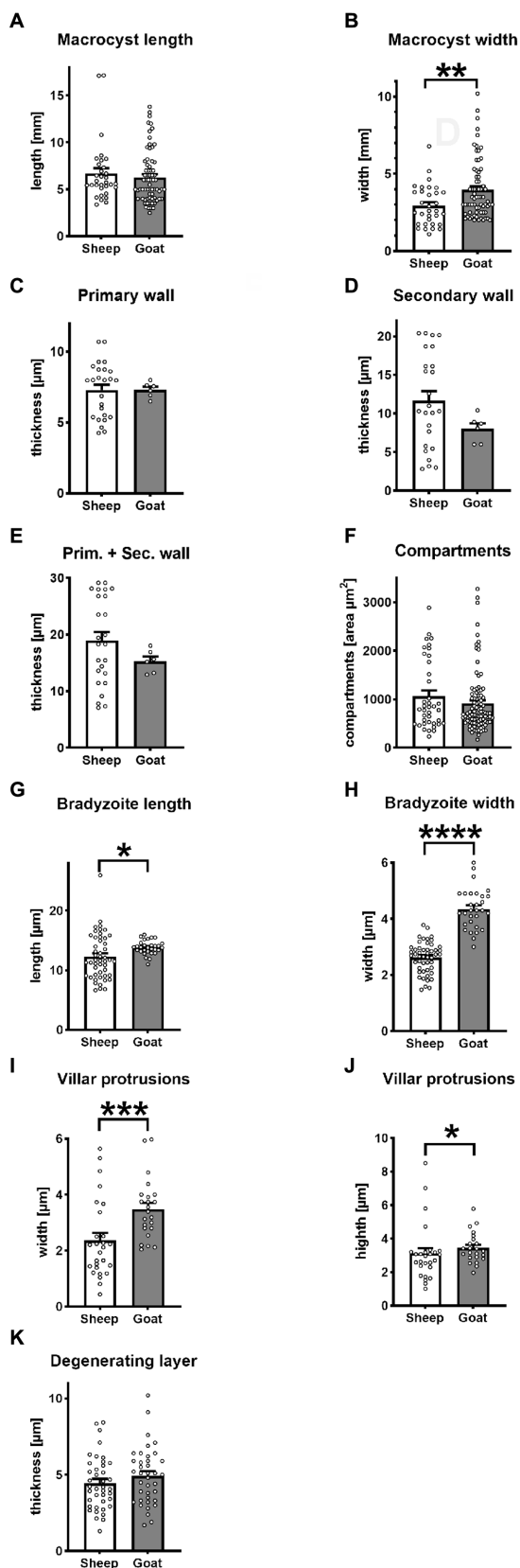


FIGURE 2
Statistical variation of macrocyst parameters between *S. gigantea* (sheep) and *S. caprafelis moulei* (goat). In all tests $p < 0.05$ was considered significant and marked with * $p < 0.01$ was assigned with

(Continued)

FIGURE 2 (Continued)

, $p < 0.001$ with *, and **** $p < 0.0001$. \pm = standard error of the mean. (A,B) macrocysts length and width: *S. gigantea* 6.7×2.9 mm, *S. caprafelis moulei* 6.3×4.0 mm ($n = 32$ sheep and $n = 70$ goat; two-tailed Mann–Whitney test). (C) Inner primary wall thickness of macrocysts: *S. gigantea* 7.3 μm , *S. caprafelis moulei* 7.3 μm . (D) Outer secondary wall thickness of macrocysts: *S. gigantea* 11.6 μm , *S. caprafelis moulei* 8.0 μm ($n = 25$ sheep, $n = 6$ goat; two-tailed Mann–Whitney test). (E) Total wall thickness of macrocysts, i.e., primary and secondary cyst walls together: *S. gigantea* 18.9 , *S. caprafelis moulei* 15.3 μm ($n = 25$ sheep, $n = 6$ goat; two-tailed Mann–Whitney test). (F) Area compartment of macrocysts: *S. gigantea* $1,065$ μm^2 , *S. caprafelis moulei* 917 μm^2 ($n = 39$ sheep, $n = 96$ goat; two-tailed Mann–Whitney test). (G) Bradyzoite length: *S. gigantea* 12.3 , *S. caprafelis moulei* 13.9 μm ($n = 49$ sheep, $n = 30$ goat; two-tailed Mann–Whitney test). (H) Bradyzoite width: *S. gigantea* 2.6 μm , *S. caprafelis moulei* 4.4 μm ($n = 49$ sheep, $n = 30$ goat; two-tailed t-test). (I) width of macrocyst villar protrusions: *S. gigantea* 2.4 μm , *S. caprafelis moulei* 3.5 μm ($n = 27$ sheep, $n = 23$ goat; two-tailed Mann–Whitney test). (J) height of macrocyst villar protrusions: *S. gigantea* 3.1 μm , *S. caprafelis moulei* 3.4 μm ($n = 27$ sheep, $n = 23$ goat; two-tailed Mann–Whitney test). (K) Thickness of the degenerating layer: *S. gigantea* 4.5 μm , *S. caprafelis moulei* 4.9 μm ($n = 40$ sheep, $n = 38$ goat; two-tailed t-test), for more details see [Supplementary material S2](#).

inner PAS-negative primary, relatively thick wall (7.3 μm in sheep and goats) was stained pale yellow in [Figures 1B,E, 2C](#). Regarding the PAS-positive outer secondary wall, it is noteworthy that Apicomplexan protozoan parasites trigger host innate immune responses *via* their cell surface glycoconjugates (22). On methylene blue staining, the secondary cyst wall appeared thick and bluish-pale in both species, whereas the primary wall was obviously thinner and purple in color. In both species, a vacuolated layer of degenerating host cells was found between the primary and secondary cyst walls ([Figures 1C,F](#)). The inner surface of the macrocysts within the primary wall was divided into a series of large round, oval or elongated compartments. The compartment sizes were approximately $1,065$ μm^2 in *S. gigantea* and 917 μm^2 in *S. caprafelis moulei* ([Figure 2F](#)). Statistical analysis revealed no significant difference ($p < 0.05$) in the thickness of macrocyst walls and sizes of compartment between sheep and goats ([Figures 2C,F](#)). Compartments were packed with banana-shaped bradyzoites with an average size of 12.3×2.6 μm in *S. gigantea* ([Figure 1C](#)), and $13.9 \mu\text{m} \times 4.4$ μm in *S. caprafelis moulei* ([Figure 1F](#)). Statistically, there is a significant difference ($p < 0.05$) in the length of bradyzoites and a highly significant difference ($p < 0.0001$) in the width of bradyzoites ([Figures 2G,H](#)) between sheep and goats. As with the macroscopical observations the differences in microscopical measurements do not allow the identification of *S. gigantea* versus *S. caprafelis moulei*, but only the source of the sample. Notably both *S. gigantea* from sheep and *S. caprafelis moulei* from goats have the same PAS-positive secondary outer cyst wall that is described here for the first time.

3.3. Ultrastructural characterization of macrosarcocysts

The *S. gigantea* and *S. caprafelis moulei* outer secondary cyst wall (PAS-positive in lightmicroscopy) consisted of a thick, fibrillar, collagenous layer, whereas the inner primary cyst wall had a homogeneous appearance. Between the secondary and primary cyst walls, was a layer of the degenerated myofibril remnants consisting of

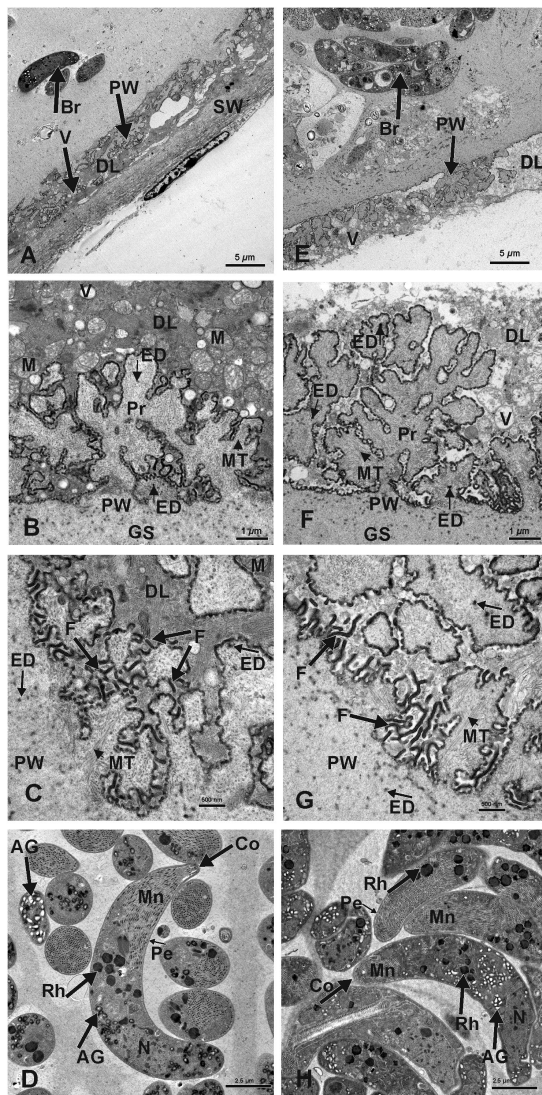


FIGURE 3

Electron micrographs of macrocysts in the esophagus of sheep (*S. gigantea*) (A–D) and goats (*S. capraefelis moulei*) (E–H). (A–C) and (E–G): showing the macrocyst wall of *S. gigantea* and *S. capraefelis moulei*, respectively. In both species, the degenerating host cells layer (DL) is located between the primary (PW) and secondary (SW) cyst walls and contains many vacuoles (V). In (E), the secondary cyst wall is absent due to mechanical damage during tissue processing. (B,C) and (F,G): High magnifications of cauliflower-like protrusions (Pr) extended from the primary to the secondary cyst wall, and numerous long dendritic-like filaments (F) protruded from both surfaces of the protrusions and the primary wall of the macrocyst. In goats (G) the protrusions are more pronounced and the filaments are slightly longer and more numerous than in sheep (C). Within the protrusions, long microtubules (MT) extended longitudinally and transversely from the core of the free protrusions into the ground substance (GS). In both species, coarse and electron-dense granules (ED) of nearly spherical in shape were observed at the base and margin of the projections and in the ground substance. (D) and (H): Ultrastructure findings of the bradyzoites of *S. gigantea* and *S. capraefelis moulei*, respectively. They exhibited a bilayered pellicle (Pe), slightly thickened at the anterior end of the banana-shaped bradyzoites and numerous small rod-shaped micronemes (Mn) with rounded ends at the anterior part (Co = conoid). Beneath the micronemes are about 8–12 irregularly shaped rhoptries (Rh), as well as some elongated tubular mitochondria and a relatively small number of amylopectin granules (AG). The cell nucleus (N) is located at the posterior end of the cell body.

numerous vacuoles of various host cell remnants. The average thickness of the degenerated layer was 4.5 μm in *S. gigantea* ($n=40$; Figures 3A,B) and 4.9 μm in *S. capraefelis moulei* ($n=38$; Figures 3E,F). Statistically, no significant difference ($p<0.05$) was observed between both species (Figure 2K). In addition, the primary macrocyst wall formed cauliflower-, trapezoid- or mushroom resembling protrusions with an average width of 2.4 μm , and a height of 3.1 μm ($n=27$, *S. gigantea*; Figure 3B). *S. capraefelis moulei* also had similar protrusion features but was slightly larger with an average width of 3.5 and height of 3.4 ($n=25$; Figures 2I,J, 3F). Statistical analysis revealed a high significant difference ($p<0.001$) in the width of villar protrusions and a significant difference ($p<0.05$) in their height between *S. gigantea* and *S. capraefelis moulei* (Figures 2I,J).

In both species, numerous dendritic-resembling filaments extended from the primary cyst-wall surface and from available surfaces of some protrusions. These filaments were significantly longer and more numerous in goats than in sheep: (Figure 3C in sheep and Figure 3G in goats)—this is the only clear morphological difference between *S. gigantea* and *S. capraefelis moulei*. Moreover, within the cauliflower-resembling protrusions, long microtubules extended longitudinally transversely from the core of the free protrusions into the ground substance of the protrusions (*S. gigantea*: Figures 3B,C; *S. capraefelis moulei*: Figures 3E,G). Coarse, spherical, electron-dense granules occurred at the base and margin of these projections and in the ground substance of the protrusions (Figures 3C,G; *S. gigantea* and *S. capraefelis moulei*, respectively). Furthermore, no marked differences in the ultrastructure of the bradyzoites were detected between these two closely related sister species.

In this study, the fine structure of *S. gigantea* cyst wall (Figures 3A–C) resembled that of the same species described previously [Figure 8.2 (C) in (1)], and the cyst wall of *S. capraefelis moulei* resembled that described briefly in previous studies [compare Figures 1–2 in (17)] with our (Figures 3E–G). In both species, the ground substance had a homogenous appearance: it formed a 3–4 μm thick septa boarder, enclosing the bradyzoites. Immediately below the primary cyst wall, some bradyzoites were visible in the ground substance. Banana-shaped bradyzoites contained a bilayered pellicle, slightly thickened at the anterior end, with a large number of small, rod-shaped micronemes” tiny, apical (23), cigar-shaped organelles involved in host cell recognition and adhesionj (23). At the anterior end of the bradyzoites, was a rounded end called a “conoid.” This is an intricate structure of spirally arranged microtubules in the apical complex of Apicomplexa that plays a role in host cell entry (cf. 23). Behind the micronemes, were approximately 8–12 irregular, varying rhoptries, along with a small amount of elongated, tubular mitochondria and amylopectin granules. Rhoptries, micronemes and electron-dense granules have previously been described as specialized secretory organelles from Apicomplexa parasites (23). The bradyzoites nucleus is mainly located at the posterior end of the body (Figure 3D in sheep, and Figure 3H in goats).

3.4. DNA-analysis

3.4.1. Molecular characterization of the 18S rDNA and sequence comparisons

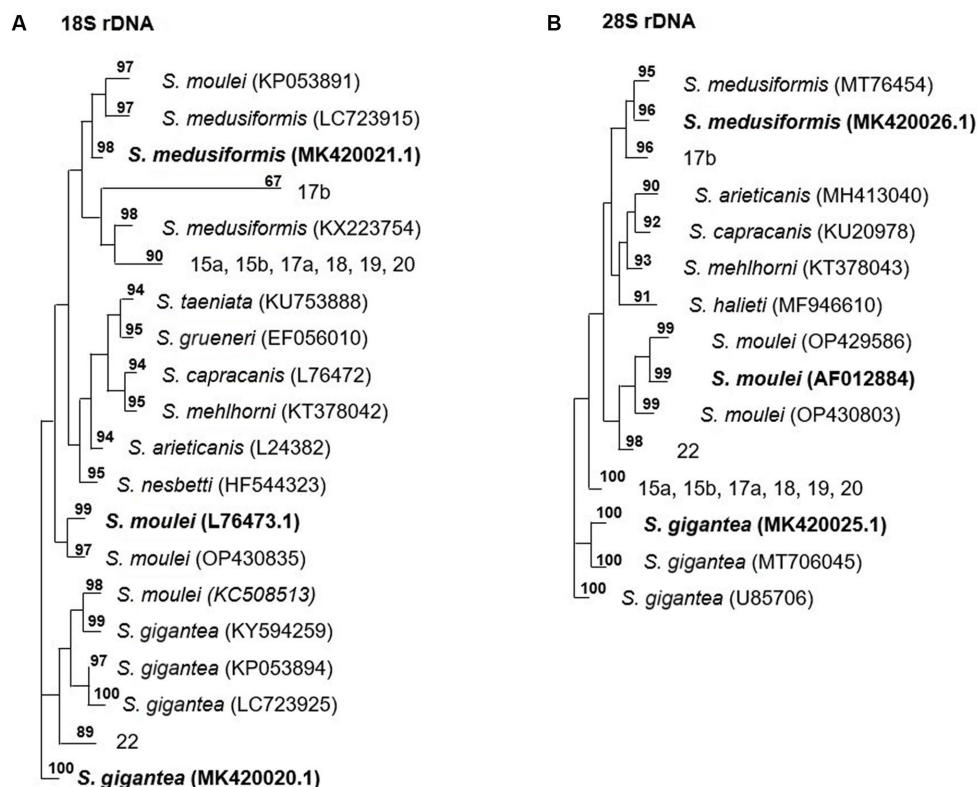
Molecularly, macrocysts from five sheep and one goat were analyzed for differences in their 18S rDNA and 28S rDNA genes. Six

TABLE 1 Sequence identity of macrocysts from sheep and goat to *Sarcocystis* spp.

Species	Gene	Accession	Sequence identity (%)							
			15a	15b	17a	17b	18	19	20	22
<i>S. gigantea</i>	18S rDNA	MK420020.1	85,2	86,1	86,0	95,6	83,5	89,1	85,5	93,5
	28S rDNA	MK420025.1	99,8	99,9	99,7	94,7	99,5	99,6	99,7	96,8
<i>S. medusiformis</i>	18S rDNA	MK420021.1	83,3	85,1	85,2	98,7	82,2	87,7	84,1	91,4
	28S rDNA	MK420026.1	95,0	95,3	95,1	99,3	95,0	95,1	95,0	94,3
<i>S. capraefelis moulei</i>	18S rDNA	L76473.1	84,7	86,0	85,8	95,6	83,1	88,7	85,0	92,9
	28S rDNA	AF012884.1	97,1	97,3	97,1	94,3	97,0	97,0	97,0	98,7

Sequence identity (%) of 3 isolated macroscopic *Sarcocystis* species with nucleotide sequences in the NCBI nucleotide databases of sheep and goats.

TABLE 2 The phylogentic tree of *Sarcocystis* spp. from sheep and goats based on18S rRNA and 28S rRNA genes.



The percentage of replicate trees in which the associated taxa were clustered together in the bootstrap test (1,000 replicates) is indicated next to the branches. Genbank accession numbers of the sequences are indicated after the taxon names.

of the seven cysts obtained from sheep (numbers: 15a, 15b, 17a, 18, 19 and 20) yielded the same 18S rDNA sequence in a multiple alignment, which was between 82.2 and 89.1% identical to the 18S rDNA genes of *S. gigantea*, *S. medusiformis* and *S. capraefelis moulei* (Tables 1, 2). Macrocyst number 17b presented the highest corresponding sequence rate with three species: 95.6, 98.7 and 95.6%, respectively. The goat-derived cyst number 22 showed between 91.4–93.5% matching sequence to the reference species. Although cysts 17b and 22 showed greater morphological similarities to *S. gigantea*, *S. medusiformis*, and *S. capraefelis moulei*, they were only 85.9% identical to each other in a pairwise alignment, indicating that the eight macrocysts were derived from three different species. In a phylogenetic tree, cyst 17b was most closely related to *S. medusiformis*, whereas cyst 22 had the farthest relation to any of the species (A in Tables 1, 2).

An NCBI nucleotide blast of the cyst sequences revealed, that the most identical sequence to cyst 17b (accession number MK420021.1), was the reference sequences used in this study for *S. medusiformis* and *S. capraefelis moulei* isolate Sarco 3 MKH 18S ribosomal RNA gene (KP053891.1) both at 99.65%. Cyst 22 was most closely matched the small subunit ribosomal RNA gene of *S. gigantea* isolate 2 (MK045326.1) with 89% sequence identity, while the six other cysts were very similar to an unknown *Sarcocystis* species HS-2009a isolate 1SO 18S ribosomal RNA gene (GQ131808.1) with 99.61% identity.

At the molecular level, using the 18S rRNA sequences, *S. gigantea* showed to be genetically related to *S. medusiformis* in sheep and *S. capraefelis moulei* in goats. The *S. gigantea* sequence was 85.1% identical to *S. medusiformis* and 80.4% identical to *S. capraefelis moulei*. In addition, *S. medusiformis* 85.9% identical to *S. capraefelis moulei*.

3.4.2. Molecular characterization of the 28S rRNA and sequence comparisons

Molecular characterization of the 28S rDNA showed that the same six macrocysts from sheep, as in the 18S rDNA analysis were highly similar in sequence and were closely related to *S. gigantea* with 99.5 to 99.9% sequence identity, followed by *S. capraefelis moulei* with 97.0 to 97.3% and *S. medusiformis* with 95.0 to 95.3% (Table 1). In contrast to the 18S rRNA, the 28S rRNA of 17b cyst sequence was less similar to *S. gigantea* (94.7%) and *S. capraefelis moulei* (94.3%), whereas it showed high similarity to *S. medusiformis*, with 99.3% sequence identity. The 28S rRNA of cyst 22 was closest to that of *S. capraefelis moulei* with 98.7%. Consistent with the 28S rRNA data of all three species, macrocysts 17b and 22 had 94.61% sequence identity.

Compared with the 18S rRNA sequence, the 28S rRNA sequence of *S. gigantea* showed closer genetic relationship to *S. medusiformis* in sheep and *S. capraefelis moulei* in goats; this sequence shared an identity of 95.4 and 97.3%, respectively. Furthermore, the new sequence of *S. medusiformis* shared an identity of 94.6% with those of *S. capraefelis moulei*.

The fact that all three randomized cyst groups have a tendency to be most identical to one of the three reference species (A in Table 2) increases the probability of the cysts originating from three different species. A nucleotide blast of the cyst sequences enhanced the pattern of the phylogenetic tree (B in Table 2), as it resulted in the three reference Accession numbers for the 28S rRNA genes used in this study.

4. Discussion

Sarcocystis species is a parasitic protozoan with a worldwide distribution, found in a variety of mammals and birds, particularly common in domestic animals. *S. gigantea* and *S. medusiformis* in sheep and *S. capraefelis moulei* in goats, which are transmitted by felids, produce macrocysts and are non-pathogenic, although they can cause poor meat quality and economic losses (24, 25). In the present study, the identification of *Sarcocystis* species is based on host specificity, cyst morphology, cyst wall and bradyzoites ultrastructural findings, and molecular characterization.

Microscopic and ultrastructural findings revealed no significant differences between *S. gigantea* and *S. capraefelis moulei* in terms of the size of macrocysts, bradyzoites, and internal compartments, as well as in the cyst wall and degeneration layer thickness. Moreover, no difference in the ultrastructural features of the bradyzoites were observed between these two closely related species. However, both species contained numerous, dendritic resembling filaments, extending from the primary cyst wall surface and from free surfaces of some protrusions. The only observable difference between the two species is the dendritic-like filaments, which are slightly longer and more numerous in goats than in sheep: (Figure 3C in sheep and Figure 3G in goats). Thus, it is difficult to distinguish these two morphologically related sister species based on ultrastructural findings alone.

Application of molecular methods showed that our DNA sequences are related to *S. gigantea* and *S. medusiformis* in sheep and *S. capraefelis moulei* in goats. In recent years, DNA analysis with high sensitivity and specificity have been used for the identification of *Sarcocystis* species. Based on previous studies, 18S rRNA and/or 28S

rRNA genes have been implemented as useful genetic markers for identification and differentiation of *Sarcocystis* in sheep (6, 12, 14, 26) and goats (12, 26).

Analysis of 28S rRNA sequences revealed that *S. gigantea* is closely related to *S. medusiformis* (95.4%) and *S. capraefelis moulei* (97.3%). In addition, our newly discovered sequence of *S. medusiformis* in sheep matched that of *S. capraefelis moulei* in goats 94.6%. Our DNA sequencing indicates that 28S rRNA sequence appear to be more suitable for identifying these species than 18S rRNA sequence.

Macroscopic sarcocystosis prevalence was reported to be 4.1% (13) in domestic sheep in Iraq, 29.3% (27), 3.3% (14) in domestic sheep in Iran and 33.6% [1991–1992; (11)] in domestic goats in Iraq and 16.6% [2004; (16)] in goats in Iran. Encouragingly, the present study showed that these infection rates decreased significantly to only 0.01% (20/141, 260) in domestic sheep and 0.02% (9/37, 399) in domestic goats during the winter season 2021–2022. Our results are confirmed by a previous study in Sulaimany province, where no macroscopic sarcocystosis was found in sheep (0.0%) in a relatively small sample only 130 tissue samples (28). In contrast, the prevalence of macroscopic sarcocystosis was remarkably higher in goats (33.6%) infected, during the winter season 1991–1992 (11), and in goats in Egypt 35.5% (15) with *S. capraefelis moulei* and originating from the same region: a slaughterhouse in Sulaimany province.

Moreover, our infection rate with *S. gigantea* in sheep (0.01%) was also remarkably lower than in sheep slaughtered in Iran in 2011 [29.3%; (28)], Romania in 2007 [26.3%, (7)], and Egypt in 2022 [42.7%; (15)].

This finding could implicate a potential improvement in animal husbandry, reflected in the very low prevalence of macroscopic sarcocystosis. An improvement in animal husbandry could have a positive impact on the general health status of the population. We believe that this improvement is due to several essential factors: (i) Establishment of new, well-organized slaughterhouses with crematoria for incinerating infected carcasses. This plays an important role in breaking the *Sarcocystis* life cycle by preventing definitive hosts from becoming infected or re-infected with *Sarcocystis* and further spreading the sporocysts. (ii) Control of stray dogs and cats, that may serve as definitive hosts by transmitting parasites to certain animal shelters or pet owners. (iii) Control of movement and transport of livestock across Kurdistan Region borders. (iv) Meat consumption of young animals (1–2 years old) due to the economic progress achieved in Iraq in the past 20 years in terms of individual income, where macroscopic sarcocystosis takes a relatively long time to develop in the muscle tissue of their intermediate hosts. (v) Television and social media, to which the Veterinary Office and the Food Control Office turn, are known to play an important role in encouraging people to improve their general knowledge about the handling and consumption of meat.

The successful application of hygienic and eradication procedures in northern Iraq Kurdistan livestock may encourage neighboring countries to adopt a similar strategy.

5. Conclusion

To our knowledge, this study is the first: (i) to reveal and describe in detail the macrocyst wall ultrastructural characteristics of *S. capraefelis moulei* in goats and compare them with those of *S. gigantea* in sheep. (ii) In which *S. medusiformis* has been isolated

from naturally infected sheep in Iraq. (iii) To investigate the influence of an appropriate hygiene strategy in animal husbandry on the prevalence of sarcocystosis in domestic animals.

Data availability statement

The data presented in the study are deposited in the GenBank NCBI nucleotide databases under the accession numbers: MK420020.1, MK420025.1, MK420021.1, MK420026.1, L76473.1, AF012884.1, KP053891.1, MK045326.1, and GQ131808.1.

Ethics statement

Ethical approval was not required for the study involving animals in accordance with the local legislation and institutional requirements because it involved the use of animal tissues obtained post mortem from animals sacrificed for non-scientific purposes. This study was conducted under the supervision of the Central Veterinary Office in Sulaimany, Kurdistan Region of Iraq, and within the framework of the regional animal protection law.

Author contributions

SN: data curation and inspection. NH: DNA-analysis, wrote a part of manuscript with contributions with MB. NP: DNA-extraction and software. TB: electron microscopy. NF-S: interpreted data. AG: interpreted data and software. WN: interpreted and analyzed data. JV: funding acquisition, interpreted data, and software. MB: data curation, electron microscopy, software, writing-original draft, and supervised this research.

Funding

This study was supported by the CRC 1451 to JV and MB and Cluster of Excellence for Aging Research (CECAD), University of Cologne, 50931, Cologne, Germany. We acknowledge support for the

References

- Dubey JP, Carlero-Bernal R, Rosenthal BM, Speer CA, Fayer R. *Sarcocystosis of animals and humans*. 2nd ed. Boca Raton, FL: CRC Press (2016).
- Heckerth AR, Tenter AM. Development and validation of species-specific nested PCRs for diagnosis of acute sarcocystosis in sheep. *Int J Parasitol*. (1999) 29:1331–49. doi: 10.1016/s0020-7519(99)00111-3
- Prakas P, Bultkauskas D, Rudaityte E, Kutkiene L, Srugosa A, Puraite I. Morphological and molecular characterization of *Sarcocystis taeniata* and *Sarcocystis pilosa* n. sp. from the sika deer (*Cervus nippon*) in Lithuania. *Parasitol Res*. (2016) 115:3021–32. doi: 10.1007/s00436-016-5057-7
- Pipia AP, Varcasia A, Zidda A, Dessi G, Panzalis R, Tamponi C, et al. Cross-sectional investigation on sheep sarcosporidiosis in Sardinia, Italy. *Vet Parasitol*. (2016) 3-4:13–7. doi: 10.1016/j.vprsr.2016.05.004
- Hoeve-Bakker BJA, Van der Giessen JWB, Franssen FFJ. Molecular identification targeting cox1 and 18S genes confirms the high prevalence of *Sarcocystis* spp. in cattle in the Netherlands. *Int J Parasitol*. (2019) 49:859–66. doi: 10.1016/j.ijpara.2019.05.008
- Gjerde B, De la Fuente C, Alunda JM, Luzon M. Molecular characterisation of five *Sarcocystis* species in domestic sheep (*Ovis aries*) from Spain. *Parasitol Res*. (2020) 119:215–31. doi: 10.1007/s00436-019-06504-6
- Adriana T, Mircean V, Blaga R, Bratu CN, Cozma V. Epidemiology and etiology in sheep *Sarcocystosis*. *Bull UASVM Vet Med*. (2008) 65:49–54.

Article Processing Charge from the DFG (German Research Foundation, 491454339). This research did not receive any specific grant from funding agencies in the public, commercial, or not-for-profit sectors.

Acknowledgments

The authors are grateful to Maruf A., director of the veterinary office of Sulaimany, Shalaw, the management of the slaughterhouse in Sulaimany, and all veterinarians in the slaughterhouses mentioned in the Kurdistan region for the providing of tissue samples. We thank Mrs. A. Jeske, university of Cologne for her skillful technical assistance and Mr. O. Parwa, Rosa travel, Cologne, Germany for his logistical support in transporting the tissue samples and M. Mohammed for his technical assistance.

Conflict of interest

The authors declare that the research was conducted in the absence of any commercial or financial relationships that could be construed as a potential conflict of interest.

Publisher's note

All claims expressed in this article are solely those of the authors and do not necessarily represent those of their affiliated organizations, or those of the publisher, the editors and the reviewers. Any product that may be evaluated in this article, or claim that may be made by its manufacturer, is not guaranteed or endorsed by the publisher.

Supplementary material

The Supplementary material for this article can be found online at: <https://www.frontiersin.org/articles/10.3389/fvets.2023.1225796/full#supplementary-material>

- Hussein NM, Hassan AA, Abd Ella OH. Morphological, ultrastructural and molecular characterization of *Sarcocystis tenella* from sheep in Qena governorate, upper Egypt. *Egypt Acad J Biol Sci*. (2018) 10:11–9. doi: 10.21608/eajbse.2018.14456
- Damboriarena PA, Silveira CS, Morais RM, Anjos BL. Natural *Sarcocystis gigantea* infection in sheep from southern Brazil. *Cienc Rural Santa Maria*. (2016) 46:1229–32. doi: 10.1590/0103-8478cr20151183
- Levine ND. The taxonomy of *Sarcocystis* (Protozoa, Apicomplexa) species. *J Parasitol*. (1986) 72:372–82. doi: 10.2307/3281676
- Barham M, Stützer H, Karanis P, Latif BM, Neiss WF. Seasonal variation in *Sarcocystis* species infections in goats in northern Iraq. *Parasitology*. (2005) 130:151–6. doi: 10.1017/s0031182004006134
- Hu JH, Liu T-T, Liu Q, Esch GW, Chen J-Q, Huang S, et al. Prevalence, morphology, and molecular characteristics of *Sarcocystis* spp. in domestic goats (*Capra hircus*) from Kunming, China. *Parasitol Res*. (2016) 115:3973–81. doi: 10.1007/s00436-016-5163-6
- Latif BM, Al-Delemi JK, Mohammed BS, Al-Bayati SM, Al-Amiry AM. Prevalence of *Sarcocystis* spp. in meat-producing animals in Iraq. *Vet Parasitol*. (1999) 84:85–90. doi: 10.1016/s0304-4017(99)00046-1
- Pestechian N, Yousefi HA, Kalantari R, Jafari R, Khamesipour F, Keshtar M, et al. Molecular and microscopic investigation of *Sarcocystis* species isolated from sheep muscles in Iran. *J Food Qual*. (2021) 2021:1–6. doi: 10.1155/2021/5562517

15. Osman FA, Gaadae HIM, Abdel-Aal SM. Some studies on *Sarcocystis* in sheep and goats in Assiut governorate Egypt. *J Parasit Dis.* (2023) 8:136. doi: 10.35841/aapddt.8.2.136
16. Shekarforoush SS, Razavi SM, Dehghan SA, Sarihi K. Prevalence of *Sarcocystis* species in slaughtered goats in shiraz, Iran. *Vet Rec.* (2005) 156:418–20. doi: 10.1136/vr.156.13.418
17. Ghaffar FA, Heydorn AO, Mehlhorn H. The fine structure of cysts of *Sarcocystis moulei* from goats. *Parasitol Res.* (1989) 75:416–8. doi: 10.1007/bf00931140
18. Bittencourt MV, Meneses IDS, Ribeiro-Andrade M, De Jesus RF, De Araújo FR, Gondim LF. *Sarcocystis* spp. in sheep and goats: frequency of infection and species identification by morphological, ultrastructural, and molecular tests in Bahia, Brazil. *Parasitol Res.* (2016) 115:1683–9. doi: 10.1007/s00436-016-4909-5
19. Schrevel J, Gros D, Monsigny M. Cytochemistry of cell glycoconjugates. *Prog Histochem Cytochem.* (1981) 14:1–254. doi: 10.1016/s0079-6336(81)80005-8
20. White DL, Mazurkiewicz JE, Barnett RJ. A chemical mechanism for tissue staining by osmium tetroxide-ferrocyanide mixtures. *J Histochem Cytochem.* (1979) 27:1084–91. doi: 10.1177/27.7.89155
21. Neiss WF. Electron staining of the cell surface coat by osmium-low ferrocyanide. *Histochemistry.* (1984) 80:231–42. doi: 10.1007/BF00495771
22. Yarovinsky F, Sher A. Toll-like receptor recognition of *Toxoplasma gondii*. *Int J Parasitol.* (2006) 36:255–9. doi: 10.1016/j.ijpara.2005.12.003
23. Mercier C, Adjogble KD, Däubener W, Delauw MF. Dense granules: are they key organelles to help understand the parasitophorous vacuole of all Apicomplexa parasites? *Int J Parasitol.* (2005) 35:829–49. doi: 10.1016/j.ijpara.2005.03.011
24. Dubey JP, Chapman JL, Rosenthal BM, Mense M, Schueler RL. Clinical *Sarcocystis neurona*, *Sarcocystis canis*, *Toxoplasma gondii*, and *Neospora caninum* infections in dogs. *Vet Parasitol.* (2006) 137:36–49. doi: 10.1016/j.vetpar.2005.12.017
25. Al-Hyali NS, Kennany ER, Khalil LY. Fate of macrosarcocysts of *Sarcocystis gigantea*. *Iraqi J Vet Sci.* (2011) 25:87–91. doi: 10.33899/ijvs.2011.5652
26. Swar SO, Shnawa BH. Ultrastructural and molecular characterization of *Sarcocystis* species derived from macroscopic sarcocysts of domestic sheep and goats in Soran City, Erbil, Iraq. *Worlds Vet J.* (2020) 10:540–50. doi: 10.36380/scil.2020.wvj65
27. Farhang-Pajuh F, Yakchali M, Mardani K. Molecular determination of abundance of infection with *Sarcocystis* species in slaughtered sheep of Urmia, Iran. *Vet Res Forum.* (2014) 5:181–6.
28. Abdullah SH. Investigation of *Sarcocystis* spp. in slaughtered cattle and sheep by peptic digestion and histological examination in Sulaimani Province, Iraq. *Vet World.* (2021) 14:468–74. doi: 10.14202/vetworld.2021.468-474